Rapid communication

W. PAA[✉]
D. MÜLLER
H. STAFAST
W. TRIEBEL

Flame turbulences recorded at 1 kHz using planar laser induced fluorescence upon hot band excitation of OH radicals

Institut für Physikalische Hochtechnologie (IPHT), Albert-Einstein-Strasse 9, 07745 Jena, Germany

ABSTRACT Laser-induced fluorescence (LIF) in flames is excited by a diode-pumped all-solid-state disk laser system which operates at a pulse repetition rate of 1 kHz and a tunable wavelength around 1030 nm. The laser fundamental is converted to 343 nm and used to excite into the hot band transition $A\,^2\Sigma^+\,(v'=0) \Leftarrow X\,^2\Pi\,(v''=1)$ of OH radicals in H_2/O_2 diffusion flames of an industrial burner and in the premixed flame of a microburner. The OH radical emission around 308 nm is resolved spectrally and spatially using a light-sheet technique. Imaging of the planar LIF (PLIF) by a gated camera visualizes the turbulent flame behavior on the millisecond time scale without averaging. To our knowledge this is the first time that an all-solid-state laser providing at the same time a kHz repetition rate as well as pulse energies of up to 5.5 mJ is available for PLIF observation of OH radicals.

1   Introduction

Laser induced fluorescence (LIF) spectroscopy has become one of the most versatile and sensitive tools for the species-selective investigation of both scientifically and technically relevant processes in the gas phase. Planar LIF (PLIF) is a particularly well established imaging method in combustion research. It is used e.g. to visualize concentration distributions in a variety of flames and combustion engines as well as around single fuel droplets or droplet arrays. LIF excitation is in most cases based on well-proven excimer laser systems or Nd:YAG laser pumped dye lasers and subsequent frequency conversion. Recently, there also have been a few LIF [1, 2] or even PLIF [3] measurements at kHz repetition rate. However, all of the latter approaches still are based upon kHz YAG lasers or copper vapor lasers with low single pulse energies for pumping the dye laser. There-

fore, the frequency-doubled output of the dye lasers is limited to energies well below 100 µJ per pulse. In addition, the complexity of such laser systems – looking at adjustments as well as installation and supporting media – remains quite high.

A significant improvement and extension of the experimental potential can, however, be achieved by diode-pumped all-solid-state lasers with pulse energies in the mJ range. Therefore, a new system based on the disk laser architecture has been developed. It is characterized by a small size and low demands for electrical and cooling power, thus enabling a mobile laser system for convenient use in technical environments. Its repetition rate in the kHz range combined with its high pulse energy allows tracking fast processes like turbulences or ignition. Its broad tunability of about 5 nm in the UV spectral region around 343 nm (upon third-harmonic generation) addresses a num-

ber of combustion-relevant species [4]. Further extensions of the applicability will arise with the generation of the fourth harmonics.

Previously, we realized PLIF measurements of formaldehyde with this novel laser system [4]. Formaldehyde is an important intermediate of the ignition process and used to probe the 'cool flame' at temperatures around 500 °C. OH radicals, on the other hand, are present only in the hot-flame regions ($T > 1000$ °C), where the steepest gradient in the concentration distribution indicates the flame front. The goal of the present work is to demonstrate that the disk laser system can be used to excite relevant LIF transitions in OH radicals.

2   Experimental

The disk laser design [5] combines the scalability to high pulse energies with an excellent beam profile needed for efficient frequency conversion to the UV spectral region. The active material Yb:YAG provides a broad tuning range (1020–1055 nm) and can be pumped by high-power laser diodes. The continuous-wave Yb:YAG seed laser operates at narrow bandwidth ($\Delta\lambda \ll 1$ pm). A Pockels cell generates short pulses (10 ns) at a repetition rate of typically 1 kHz (up to 4 kHz). These spectrally and temporally well defined pulses are amplified in a regenerative amplifier, which also exploits the disk laser architecture. After amplification pulse energies of up to 25 mJ with identical spectral properties yield a mean average power of 25 W. In the final stage the laser fundamental of around 1030 nm is converted to around 343 nm (third harmonic) and shaped to a light

✉ Fax: +49-3641-206-499, E-mail: wolfgang.paa@ipht-jena.de

sheet inside the flame. Pulse energies of up to 5.5 mJ at 1 kHz are available to excite selectively the fluorescence of formaldehyde or OH radicals. Since neither the amplification process nor the frequency-conversion stages lead to a spectral broadening, the laser line width still amounts to much less than 1 pm also at 343 nm. This value only represents an upper limit arising from the highest available accuracy of our wavemeter. The smallest tuning step corresponds to the axial mode separation of 1.6 pm at the fundamental, i.e. 0.53 pm for the third harmonic. A more detailed description of the laser and its potential applications can be found in the literature [4, 6, 7].

OH radicals are created in the H_2/O_2 diffusion flame of an industrial burner and in a premixed flame of a newly developed microburner. With the industrial burner both gases are emitted from concentric nozzles, while the microburner benefits from etched microstructures inside a small glass chip used to premix the gases.

The emission at 308 nm is detected using a short-pass filter with an edge at 320 nm to suppress scattered laser light (343 nm). PLIF is recorded by a Photron FastCam Ultima APX I^2 camera system. It consists of a 10-bit, 1024×1024 pixel fast-scan CMOS sensor and a dual-stage image intensifier which is sensitive in the UV spectral region. Up to 2000 single frames per second are possible without loss in spatial or temporal resolution and without averaging over laser pulses. The image intensifier of the camera is gated electronically to a width of typically 100 ns. The spectrally resolved measurements are performed with an intensified slow-scan 16-bit CCD camera system (PI-MAX, Roper Scientific) connected to a spectrograph providing a spectral resolution < 0.1 nm.

3   Selection of optical OH transitions

The excitation of OH radicals within the electronic transition $A\,^2\Sigma^+ - X\,^2\Pi$ is conveniently performed via the transitions ($v' = 0$, $v'' = 0$) at 308 nm, (1, 0) at 282 nm, and (3, 0) at 248 nm [8]. At 308 nm ((0, 0) transition), however, the wavelengths for absorption and fluorescence overlap strongly, so that this transition is hardly used in recent

experiments. The (3, 0) transition at 248 nm, on the other hand, populates a predissociative state showing a low fluorescence yield. With (1, 0) excitation at 282 nm vibrational relaxation of the emitting state ($v' = 1$) has to be considered.

Here, we consider the hot band transition ($v' = 0$, $v'' = 1$) located at 343 nm for excitation and the (0, 0) transition at 308 nm for detection as an attractive alternative. The relative transition probabilities at 308 nm (0, 0), 282 nm (1, 0), 248 nm (3, 0), and 343 nm (0, 1) amount to 1000, 334, 11, and 4, respectively [8]. Despite the three times lower transition probability compared with the (3, 0) transition (ratio 4 : 11), the long lifetime and high fluorescence quantum yield of the ($v' = 0$) state should yield a higher fluorescence signal than that from the ($v' = 3$) state. An additional advantage is that vibrational relaxation of ($v' = 0$) need not be considered. The hot band nature of the selected (0, 1) transition also offers the possibility to investigate the OH ($v'' = 1$) concentration in the flames. This may be attractive for future applications because considerable deviations from the Boltzmann distribution were revealed by cavity ring-down spectroscopy in special methane flames and amounted to a factor of up to 20 [9].

Using the software package Lif-Base [10] we found that efficient excitation is possible at $\lambda_{Exc.} = 343.598$ nm (air) via $A\,^2\Sigma^+$ ($v' = 0$) $\leftarrow X\,^2\Pi$ ($v'' =$

1), hitting two rovibronic transition lines $R_2(10)$ and $R_1(7)$ located within 0.2 pm (resolution limit of LifBase). Emission via the (0, 2) transition around 395 nm should be very weak. The strong ($v' = 0$) $\rightarrow$ ($v'' = 1$) emission around 350 nm, on the other hand, is very close to the excitation wavelength so that custom-made filters with extremely sharp edges would be necessary. Therefore, we selected the (0, 0) transition band for LIF recording, which is placed on the anti-Stokes side around 308 nm and sufficiently separated from the excitation wavelength.

4   Results and discussion

The characteristic emission spectrum of OH radicals around 308 nm ($A\,^2\Sigma^+$ ($v' = 0$) $\rightarrow X\,^2\Pi$ ($v'' = 0$)) obtained with the industrial burner flame was corrected for the sensitivity of the detection system (imaging lenses, spectrometer, intensifier, and camera) and is shown in Fig. 1. Its high sensitivity to detuning of the excitation wavelength confirmed that we excited resonantly into narrow-band transitions of the OH radicals. A series of prominent rovibronic transitions appeared, e.g. at 309.4, 310.7, 312.4, and 314.8 nm (marked in Fig. 1), which are clearly visible as peaks in the spectrum. For the interpretation of this result two methods of spectrum simulation are applied successively.
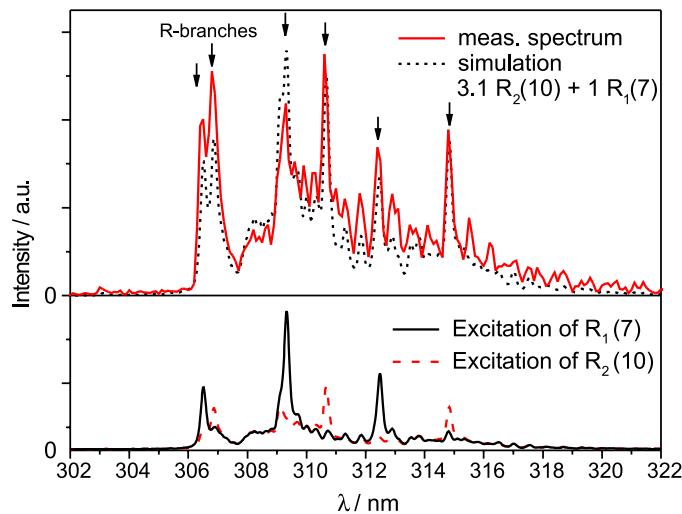
FIGURE 1   LIF emission spectrum of OH radicals recorded with the industrial burner upon excitation at $\lambda_{Exc.} = 343.598$ nm, $E = 3.7$ mJ/pulse (*top*, *solid line*, accumulation of 100 laser pulses) and calculated with the LasKin software (*top*, *dashed line*). The calculated spectrum is the superposition of two spectra after excitation of the $R_2(10)$ transition (*bottom*, *solid line*) and the $R_1(7)$ transition (*bottom*, *dashed line*)

For the first simulation of the spectrum LifBase was employed assuming thermalization (Boltzmann distribution) of the rotational states within the $A\,^2\Sigma^+$ ($v' = 1$) state (not shown here). It yields precisely the spectral positions while significant deviations remain in the intensity distribution. Particularly, the above-mentioned peaks appear with relatively low intensity. Assigning the single peaks to individual rovibronic transitions indicates, however, that they originate mainly from rotational levels excited by the laser pulse (rotational quantum numbers $N' = 11$, $R_2(10)$ and $N' = 8$, $R_1(7)$). Therefore, it is concluded that the fluorescence spectrum approximately reflects the superposition of a highly non-thermal initial population (only $N' = 8$ and $N' = 11$ are optically populated) and the rotational relaxation to a Boltzmann distribution within the recording time of the spectrum (about 500 ns).

Subsequently, we tried to model the relaxation quantitatively. We used a program called LasKin [11] to simulate the time-resolved spectra or – more precisely – the integration over a dynamically changing fluorescence spectrum due to rotational and vibrational relaxation and quenching. The excited rovibronic transition lines $R_2(10)$ and $R_1(7)$ are extremely close (Sect. 3). Taking into account the rate of rotational energy transfer in the order of 10^{10} s^{-1}, the collisionally broadened line widths amount to 1.5 pm. As a result, the excitation via the $R_2(10)$ and $R_1(7)$ lines cannot be separated. This satisfies the assumption that the excitation laser pulse populates the $N' = 8$ as well as the $N' = 11$ states. The recorded fluorescence spectrum is the weighted superposition of both emission spectra. The best agreement between the simulated spectrum and our data can be obtained by adding the individual spectra after $R_2(10)$ and $R_1(7)$ excitation (Fig. 1, bottom) in the ratio of 3.1:1 (dashed line in the upper part of Fig. 1).

There remain, however, deviations between the simulated and the measured spectra for the peaks belonging to the R branches (306–307 nm). These are attributed to the facts that: (i) the temperature varies strongly across the field of detection, i.e. the spectrum results from an ensemble of OH radicals with an inhomogeneous temperature distribution, (ii) self-absorption varies locally due to flame geometry, and (iii) the calculations were performed for OH radicals only, although LasKin is capable of handling collisions with different atoms/molecules (e.g. OH, O, O_2, H, H_2, H_2O, and N_2). The contributions of these species are, however, unknown so far.

Within the following experiments two-dimensional spatially resolved LIF (PLIF) was recorded using the light-sheet technique. Figure 2 shows a sequence of six consecutive frames at 1 ms time resolution with the laser operating at a pulse energy of 3.7 mJ. Particularly in the center of the flame above the inner concentric nozzle a turbulent behavior of the OH concentration distribution is observed.

The laser light sheet of approximately 11 mm height was located closely above the concentric burner nozzles (20 mm), so that the structure of the PLIF image is influenced by the separated inlets of the oxidizer (O_2) and fuel (H_2). The bright areas – showing a high concentration of OH radicals – visualize hot regions in the flame, while the steep gradient of the concentration distribution indicates the flame front. Comparing the single frames within the sequence in Fig. 2, the outer parts of the flame appear to be rather stable, while the inner parts show a turbulent behavior.

The flame of the industrial burner extends to a total height of more than 50 cm. We selected heights of 20 mm, 50 mm, and 150 mm to record PLIF images. For each height one typical image without additional averaging (Fig. 3) illustrates the variation of the OH radical distribution. As expected, the OH concentration becomes more and more homogeneous with increasing height above the nozzles. Consequently, structures which are clearly visible at a height of 20 mm change to a more uniform distribution at 150 mm.

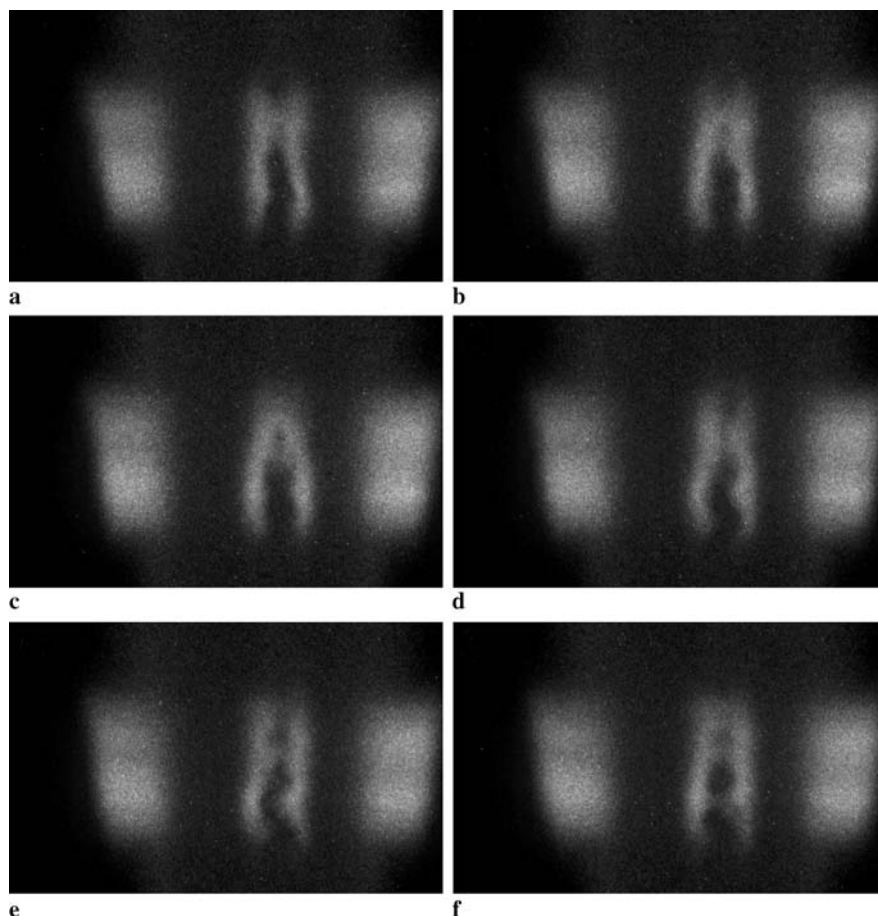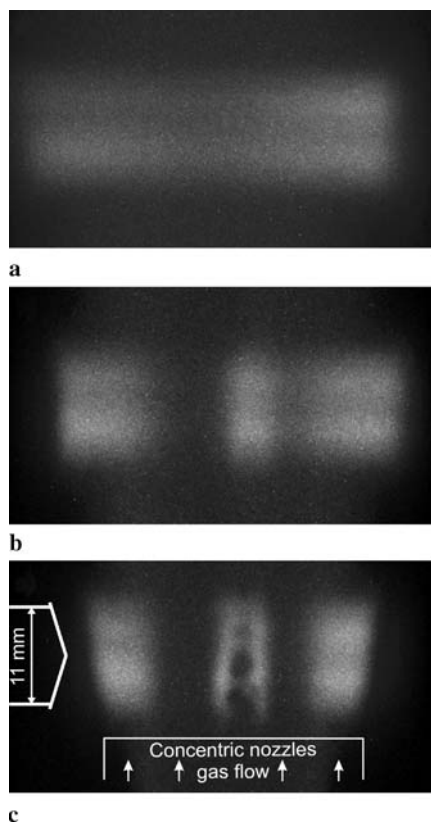To compare the hot band excitation with the more common excitation via

FIGURE 2   Six consecutive frames ($\Delta t = 1$ ms) from a movie of 2000 single frames, showing PLIF of OH in a flame region close to the nozzles of the industrial burner ($E = 3.7$ mJ/pulse)

FIGURE 3   PLIF images (**a**, **b**, and **c**) of OH radicals in the H_2/O_2 diffusion flame at heights of 150, 50, and 20 mm above the nozzles of the industrial burner. Also marked in image (**c**): direction/height of light sheet (*left*) and position of concentric nozzles (*bottom*)

the (3, 0) band at 248 nm, we repeated the above experiment under identical experimental conditions (same parameters of the burner, the camera, the gain factor of the camera/intensifier system, and the height of the light sheet) with the solid-state-laser replaced by a KrF excimer laser with pulse energy of 6.5 mJ. Images of about the same intensity (counts per pixel) as before were obtained. This finding deserves some comment: the calculated Boltzmann population densities for different flame temperatures are given in Table 1. It shows that for excitation of the (3, 0) $P_2(8)$ transition ($v'' = 0$, $N'' = 8$) about 10 times more molecules than for the (0, 1) $R_2(10)$ or $R_1(7)$ transition with ($v'' = 1$, $N'' = 7$ or $N'' = 10$) are available in the initial state. As mentioned above, the transition probability of the (3, 0) band is at least three times higher than that of (0, 1) [8]. Multiplying these three factors (pulse energy, population numbers, and transition probability) yields a total factor of approximately 60 in favor of the (3, 0) excitation. The fact that we
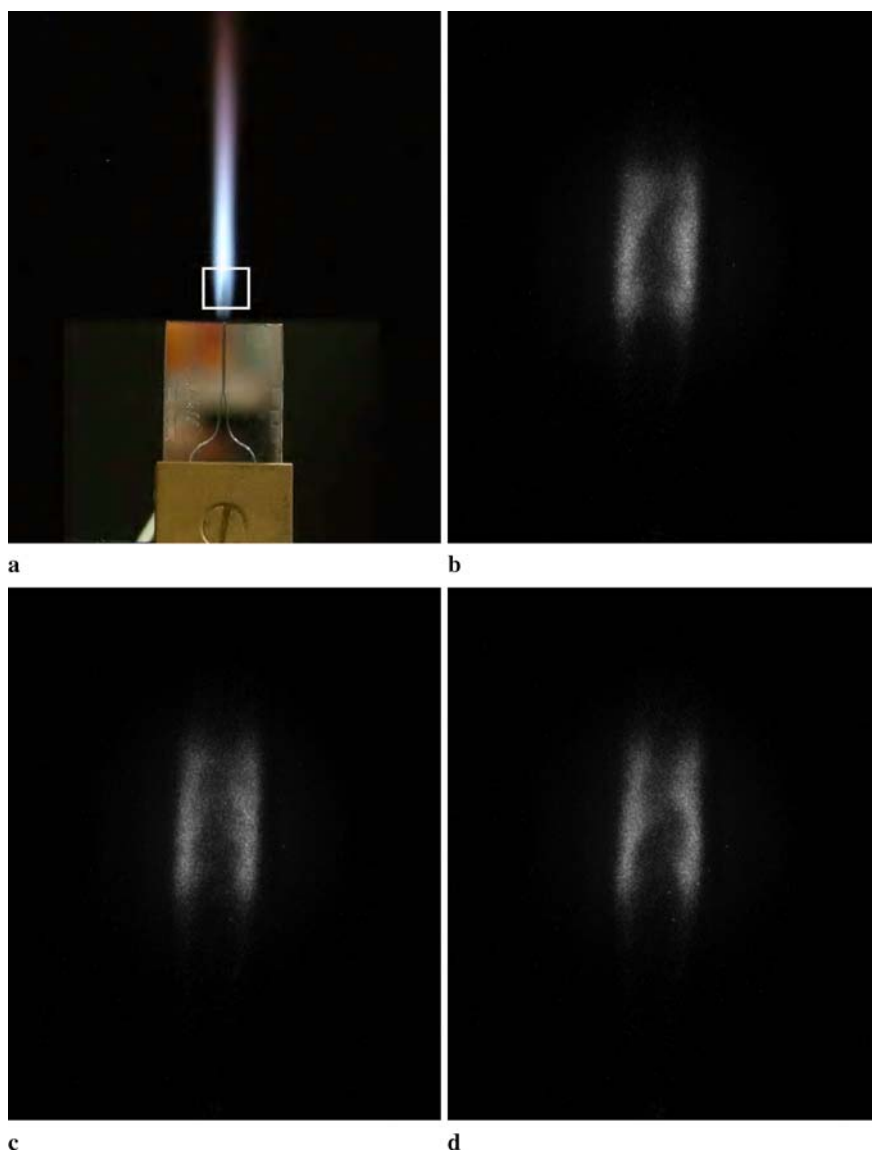
FIGURE 4   Photograph of the microburner with flame (**a**) and consecutive PLIF images (**b**, **c**, and **d**) of OH radicals in the H_2/O_2 premixed flame above the newly developed microburner. The *white rectangle* in (**a**) indicates the area of the PLIF images

T/K	Ground state ($v'' = 0$)		First excited state ($v'' = 1$)		
	total	$N = 8$	total	$N = 7$	$N = 10$
1500	0.967	0.082	0.032	0.0031	0.0018
2000	0.923	0.080	0.071	0.0066	0.0047
2500	0.870	0.073	0.111	0.0095	0.0078
3000	0.816	0.064	0.147	0.0012	0.0010

TABLE 1   Relative Boltzmann population densities of the initial states ($v'' = 0$, $N = 8$), ($v'' = 1$, $N = 7$), and ($v'' = 1$, $N = 10$) calculated for selected temperatures. These states are used for exciting the transitions (3, 0) $P_2(8)$, (0, 1) $R_2(10)$, and (0, 1) $R_1(7)$

nevertheless observe the same emission intensities can be attributed to the excitation efficiency with the very narrow line width of the disk laser (< 1 pm) compared to that of the excimer laser (2 pm) and to the small emission quantum yield of the $A^2\Sigma^+$ ($v' = 3$) level due to its predissociative nature.

Finally, using the same laser parameters as before (343.598 nm, and 3.7 mJ/pulse), the flame of a newly developed microburner was subject to PLIF measurements with the first results shown in Fig. 4. In this case fuel (H_2) and oxidizer (O_2) are premixed inside a microstructured glass chip. The

mixture is ignited at the exit of the chip (200 µm in diameter) and forms a turbulent flame with a height of $1-2$ cm. PLIF with a kHz frame rate provides a convenient tool to optimize both the operational parameters and the microstructure of the chip to achieve a homogeneous fuel/air mixture and a stable flow and combustion regime.

5   Summary and conclusions

The Yb:YAG thin disk laser system developed for PLIF applications proved to be a powerful new tool for laser diagnostics in combustion research. LIF/PLIF measurements of OH radicals – a very important species in all hot combustion processes – were successfully demonstrated. Taking advantage of the kHz repetition rate, it is now possible to track fast processes and turbulences down to the millisecond time scale with an all-solid-state laser. Exciting OH radicals via the hot band transition $A\,^2\Sigma^+\,(v'=0) \leftarrow X\,^2\Pi\,(v''=1)$ and recording of LIF/PLIF around 308 nm ((0, 0) transition), it has become possible to obtain results similar to those gained with excimer or dye lasers which are commonly used in combustion research. Moreover, the selected hot band excitation can be used in further experiments to investigate non-equilibrium

distributions of OH radicals which are reflected in the emission spectrum.

Based on its unique parameters (tunability, narrow bandwidth, and kHz repetition rate) the new all-solid-state laser may substitute and/or complement excimer and dye laser based diagnostics. To reach this goal, transitions with higher fluorescence quantum yield will be investigated in the near future. The fourth harmonics of the laser around 260 nm will allow us to excite the (2, 0) band with a transition probability 15 times higher than that of the (0, 1) band [8]. Furthermore, flames with other fuel/oxidizer compositions, i.e. lower OH concentrations, also have to be examined.

As an important application example, the new solid-state laser system will be integrated into a drop capsule for drop-tower applications at Bremen, since experiments under microgravity conditions are playing an important role in combustion research. The experiments at the drop tower may also stimulate a laser system designed for PLIF and other laser diagnostic techniques onboard the International Space Station (ISS).

REFERENCES

1   D.E. Heard, M.J. Pilling, Chem. Rev. **103**, 5163 (2003)
2   Y. Kanaya, H. Akimoto, Appl. Opt. **45**, 1254 (2006)
3   J. Wäsle, A. Winkler, T. Sattelmayer, Flow Turbul. Combust. **75**, 29 (2005)
4   W. Paa, D. Müller, A. Gawlik, W. Triebel, in *Proc. SPIE 5880*, San Diego, CA, 2005, paper no. 58800N-1
5   A. Giesen, H. Hügel, A. Voss, K. Wittig, U. Brauch, H. Opower, Appl. Phys. B **58**, 365 (1994)
6   M. Larionov, C. Stolzenburg, A. Giesen, W. Paa, W. Triebel, C. Eigenbrod, presentation at *CLEO Europe*, Munich (2005), paper CA3-1-TUE
7   A. Baum, D. Grebner, W. Paa, W. Triebel, M. Larionov, A. Giesen, Appl. Phys. B **81**, 1091 (2005)
8   D.R. Crosley, R.K. Lengel, J. Quantum. Spectrosc. Radiat. Transf. **15**, 579 (1975)
9   V.A. Lozovsky, I. Derzy, S. Cheskis, Chem. Phys. Lett. **284**, 407 (1998)
10 J. Luque, D.R. Crosley, *LIFBASE: Database and Spectral Simulation Program*, Version 2.0.53, SRI International Rep. MP 99-009 (1999)
11 U. Rahmann, A. Bülter, U. Lenhard, R. Düsing, D. Markus, A. Brockhinke, K. Kohse-Höinghaus, *LASKIN – A Simulation Program for Time-Resolved LIF-Spectra*, Internal Rep., University of Bielefeld, Faculty of Chemistry, Physical Chemistry I [http://pc1.uni-bielefeld.de/~laskin]